

Chapter 2

Nanoindentation Testing

2.1 Nanoindentation Test Data

The goal of the majority of nanoindentation tests is to extract elastic modulus and hardness of the specimen material from load-displacement measurements. Conventional indentation hardness tests involve the measurement of the size of a residual plastic impression in the specimen as a function of the indenter load. This provides a measure of the area of contact for a given indenter load. In a nanoindentation test, the size of the residual impression is often only a few microns and this makes it very difficult to obtain a direct measure using optical techniques. In nanoindentation testing, the depth of penetration beneath the specimen surface is measured as the load is applied to the indenter. The known geometry of the indenter then allows the size of the area of contact to be determined. The procedure also allows for the modulus of the specimen material to be obtained from a measurement of the “stiffness” of the contact, that is, the rate of change of load and depth. In this chapter, the mechanics of the actual indentation test and the nature of the indenters used in this type of testing are reviewed.

2.2 Indenter Types

Nanoindentation hardness tests are generally made with either spherical or pyramidal indenters. Consider a Vickers indenter with opposing faces at a semi-angle of $\theta=68^\circ$ and therefore making an angle $\beta=22^\circ$ with the flat specimen surface. For a particular contact radius a , the radius R of a spherical indenter whose edges are at a tangent to the point of contact with the specimen is given by $\sin \beta=a/R$, which for $\beta=22^\circ$ gives $a/R=0.375$. It is interesting to note that this is precisely the indentation strain¹ at which Brinell hardness tests, using a spherical indenter, are generally performed, and the angle $\theta=68^\circ$ for the Vickers indenter was chosen for this reason.

¹ Recall that the term “indentation strain” refers to the ratio a/R .

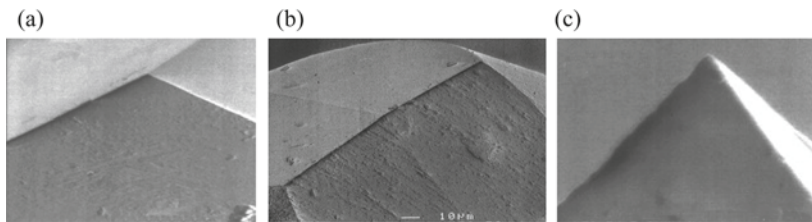


Fig. 2.1 SEM images of the tips of (a) Berkovich, (b) Knoop, and (c) cube-corner indenters used for nanoindentation testing. The tip radius of a typical diamond pyramidal indenter is in the order of 100 nm. (Courtesy Fischer-Cripps Laboratories)

The Berkovich indenter [1], (a) in Fig. 2.1, is generally used in small-scale indentation studies and has the advantage that the edges of the pyramid are more easily constructed to meet at a single point, rather than the inevitable line that occurs in the four-sided Vickers pyramid. The face angle of the Berkovich indenter normally used for nanoindentation testing is 65.27° , which gives the same projected area-to-depth ratio as the Vickers indenter. Originally, the Berkovich indenter was constructed with a face angle of 65.03° , which gives the same *actual* surface area to depth ratio as a Vickers indenter. The tip radius for a typical new Berkovich indenter is on the order of 50–100 nm. This usually increases to about 200 nm with use. The Knoop indenter, (b) in Fig. 2.1, is a four-sided pyramidal indenter with two different face angles. Measurement of the unequal lengths of the diagonals of the residual impression is very useful for investigating anisotropy of the surface of the specimen. The indenter was originally developed to allow the testing of very hard materials where a longer diagonal line could be more easily measured for shallower depths of residual impression. The cube corner indenter, (c) in Fig. 2.1, is finding increasing popularity in nanoindentation testing. It is similar to the Berkovich indenter but has a semi-angle at the faces of 35.26° .

Conical indenters have the advantage of possessing axial symmetry, and, with reference to Fig. 2.1, equivalent projected areas of contact between conical and pyramidal indenters are obtained when:

$$A = \pi h_c^2 \tan^2 \alpha \quad (2.1)$$

where h_c is depth of penetration measured from the edge of the circle or area of contact. For a Vickers or Berkovich indenter, the projected area of contact is $A = 24.5h_c^2$ and thus the semi-angle for an equivalent conical indenter is 70.3° . It is convenient when analyzing nanoindentation test data taken with pyramidal indenters to treat the indentation as involving an axial-symmetric conical indenter with an apex semi-angle that can be determined from Eq. 2.1. Table 1.1 gives expressions for the contact area for different types of pyramidal indenters in terms of the penetration depth h_c for the geometries shown in Fig. 2.2.

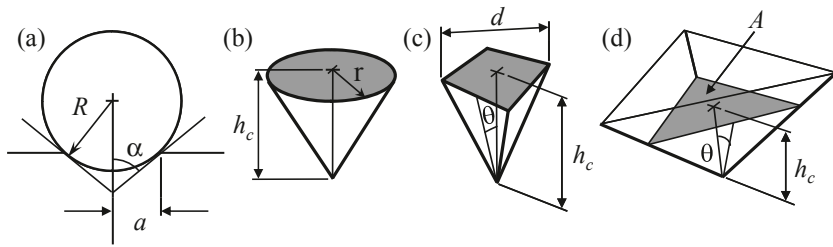
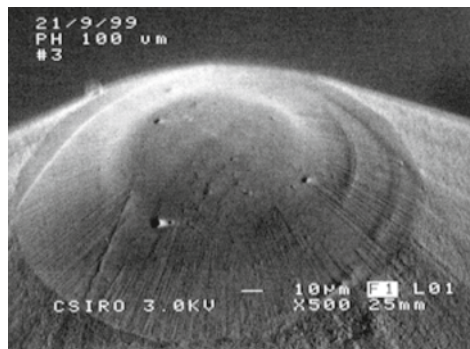


Fig. 2.2 Indentation parameters for (a) spherical, (b) conical, (c) Vickers, and (d) Berkovich indenters (not to scale)

Fig. 2.3 Tip of a sphero-conical indenter used for nanoindentation and scratch testing. Nominal tip radius is 100 μm in this example. Tip radii of $<1\ \mu\text{m}$ are available. (Courtesy CSIRO)



Spherical indenters are finding increasing popularity, as this type of indenter provides a smooth transition from elastic to elastic–plastic contact. It is particularly suitable for measuring soft materials and for replicating contact damage in in-service conditions. As shown in Fig. 2.3, the indenter is typically made as a sphero-cone for ease of mounting. Only the very tip of the indenter is used to penetrate the specimen surface in indentation testing. Diamond spherical indenters with a radius of less than 1 micron can be routinely fashioned.

Indenters can generally be classified into two categories—sharp or blunt. The criteria upon which a particular indenter is classified, however, are the subject of opinion.

For example, some authors [2] classify sharp indenters as those resulting in permanent deformation in the specimen upon the removal of load. A Vickers diamond pyramid is such an example in this scheme. However, others prefer to classify a conical or pyramidal indenter with a cone semi-angle $\alpha > 70^\circ$ as being blunt. Thus, a Vickers diamond pyramid with $\theta = 68^\circ$ would in this case be considered blunt. A spherical indenter may be classified as sharp or blunt depending on the applied load according to the angle of the tangent at the point of contact. The latter classification

is based upon the response of the specimen material in which it is observed that plastic flow according to the slip-line theory occurs for sharp indenters and the specimen behaves as a rigid-plastic solid. For blunt indenters, the response of the specimen material follows that predicted by the expanding cavity model or the elastic constraint model, depending on the type of specimen material and magnitude of the load. Generally speaking, spherical indenters are termed blunt, and cones and pyramids are sharp.

2.3 Indentation Hardness and Modulus

A particularly meaningful quantity in indentation hardness is the mean contact pressure of the contact, and is found by dividing the indenter load by the projected area of the contact. The mean contact pressure, when determined under conditions of a fully developed plastic zone, is usually defined as the “indentation hardness” H_{IT} of the specimen material. In nanoindentation testing, the displacement of the indenter is measured and the size of the contact area (at full load) is estimated from the depth of penetration with the known geometry of the indenter. For an extreme case of a rigid-plastic solid, where there is little elastic recovery of material, the mean contact pressure at a condition of a fully developed plastic zone is a true representation of the resistance of the material to permanent deformation. When there is substantial elastic recovery, such as in ceramics where the ratio of E/H is low, the mean contact pressure, at a condition of a fully developed plastic zone, is not a true measure of the resistance of the material to plastic deformation but rather measures the resistance of the material to combined elastic and plastic deformations. The distinction is perhaps illustrated by a specimen of rubber, which might deform elastically in an indentation test but undergo very little actual permanent deformation. In this case, the limiting value of mean contact pressure (the apparent indentation hardness) may be very low but the material is actually very resistant to permanent deformation and so the true hardness is very high. The distinction between the true hardness and the apparent hardness is described in more detail in Chap. 3.

In depth-sensing indentation techniques used in nanoindentation, the elastic modulus of the specimen can be determined from the slope of the unloading of the load-displacement response. The modulus measured in this way is formally called the “indentation modulus” E_{IT} of the specimen material. Ideally, the indentation modulus has precisely the same meaning as the term “elastic modulus” or “Young’s modulus” but this is not the case for some materials. The value of indentation modulus may be affected greatly by material behavior (e.g. piling-up) that is not accounted for in the analysis of load-displacement data. For this reason, care has to be taken when comparing the modulus for materials generated by different testing techniques and on different types of specimens.

2.3.1 Spherical Indenter

The mean contact pressure, and, hence, indentation hardness, for an impression made with a spherical indenter is given by:

$$p_m = H = \frac{P}{A} = \frac{4P}{\pi d^2} \quad (2.2)$$

where d is the diameter of the contact circle at full load (assumed to be equal to the diameter of the residual impression in the surface). In nanoindentation testing, it is usual to find that the size of the residual impression is too small to be measured accurately with conventional techniques and instead, the contact depth (h_c as shown in Fig. 1.1) and the area of contact calculated using the known geometry of the indenter. For a spherical indenter, the area of contact is given by:

$$\begin{aligned} A &= \pi (2R_i h_c - h_c^2) \\ &\approx 2\pi R_i h_c \end{aligned} \quad (2.3)$$

where the approximation is appropriate when the indentation depth is small compared to the radius of the indenter.

The mean contact pressure determined from Eq. 2.2 is based on measurements of the projected area of contact and is often called the “Meyer” hardness H . By contrast, the Brinell hardness number (BHN) uses the actual area of the curved surface of the impression and is found from:

$$BHN = \frac{2P}{\pi D(D - \sqrt{D^2 - d^2})} \quad (2.4)$$

where D is the diameter of the indenter. The Brinell hardness is usually performed at a value for a/R (the indentation strain) of 0.4, a value found to be consistent with a fully developed plastic zone. The angle of a Vickers indenter (see Sect. 2.3.2 below) was chosen originally so as to result in this same level of indentation strain.

The use of the area of the actual curved surface of the residual impression in the Brinell test was originally thought to compensate for strain-hardening of the specimen material during the test itself. However, it is now more generally recognized that the Meyer hardness is a more physically meaningful concept.

Meyer found that there was an empirical size relationship between the diameter of the residual impression and the applied load, and this is known as Meyer’s law:

$$P = kd^n \quad (2.5)$$

In Eq. 2.4, k and n are constants for the specimen material. It was found that the value of n was insensitive to the radius of the indenter and is related to the strain-hardening exponent x of the specimen material according to

$$n = x + 2 \quad (2.6)$$

Values of n were found to be between 2 and 2.5, the higher the value applying to annealed materials, while the lower value applying to work-hardened materials (low value of x in Eq. 2.5). It is important to note that Meyer detected a lower limit to the validity of Eq. 2.4. Meyer fixed the lower limit of validity to an indentation strain of $a/R=0.1$. Below this, the value of n was observed to increase—a result of particular relevance to nanoindentation testing.

2.3.2 Vickers Indenter

For a Vickers diamond pyramid indenter (a square pyramid with opposite faces at an angle of 136° and edges at 148° and face angle 68°), the Vickers diamond hardness, VDH , is calculated using the indenter load and the actual surface area of the impression. The VDH is lower than the mean contact pressure by $\approx 7\%$. The Vickers diamond hardness is found from:

$$VDH = \frac{2P}{d^2} \sin \frac{136^\circ}{2} = 1.8544 \frac{P}{d^2} \quad (2.7)$$

with d equal to the length of the diagonal measured from corner to corner on the residual impression in the specimen surface. Traditionally, Vickers hardness is calculated using Eq. 2.7 with d in mm and P in kgf^2 . The resulting value is called the Vickers hardness and given the symbol HV . The mean contact pressure, or Meyer hardness, is found using the projected area of contact, in which case we have:

$$p_m = H = 2 \frac{P}{d^2} \quad (2.8)$$

There is a direct correspondence between HV and the Meyer hardness H . To convert Meyer hardness to HV , we write:

$$\begin{aligned} HV &= 1.8544 \frac{P}{d^2} \\ H &= \frac{2(\text{kgf})(9.81)}{d^2} \\ \text{kgf} &= \frac{Hd^2}{2(9.81)} \\ HV &= \frac{1.8544}{d^2} \frac{Hd^2}{2(9.81)} \\ &= \frac{1.854}{2(9.81)} H \\ &= 0.094495 H \end{aligned} \quad (2.9)$$

² 1 kgf = 9.806 N.

where we have used 9.81 for acceleration due to gravity and H is in $\text{N/mm}^2 = \text{MPa}$.

In nanoindentation testing, the area of contact is found from a determination of the contact depth h_c . The projected area of contact is given by:

$$\begin{aligned} A &= 4h_c^2 \tan^2 68 \\ &= 24.504 h_c^2 \end{aligned} \quad (2.10)$$

In contrast, in terms of the contact depth h_c , the actual area of contact is given by:

$$A = \frac{4 \sin \theta}{\cos^2 \theta} h_c^2 \quad (2.11)$$

where for $\theta = 68^\circ$ we have $A \approx 26.42865 h_c^2$. From geometry, it is easy to show that the length of the diagonal of the residual impression is larger than the total depth of penetration by a factor of precisely 7.

2.3.3 Berkovich Indenter

The Berkovich indenter is used routinely for nanoindentation testing because it is more readily fashioned to a sharper point than the four-sided Vickers geometry, thus ensuring a more precise control over the indentation process. The mean contact pressure is usually determined from a measure of the contact depth of penetration, h_c in (see Fig. 1.3), such that the projected area of the contact is given by:

$$A = 3\sqrt{3}h_c^2 \tan^2 \theta \quad (2.12)$$

which for $\theta = 65.27^\circ$, evaluates to:

$$\begin{aligned} A &= 24.494 h_c^2 \\ &\approx 24.5 h_c^2 \end{aligned} \quad (2.13)$$

and hence the mean contact pressure, or hardness, is:

$$H = \frac{P}{24.5 h_c^2} \quad (2.14)$$

The original Berkovich indenter was designed to have the same ratio of actual surface area to indentation depth as a Vickers indenter and had a face angle of 65.0333° . Since it is customary to use the mean contact pressure as a definition of hardness in nanoindentation, Berkovich indenters used in nanoindentation work are designed to have the same ratio of projected area to indentation depth as the Vickers indenter in which case the face angle is 65.27° . The equivalent cone angle (which gives the same area to depth relationship) is 70.296° . From geometry, the ratio of the length of one side of the residual impression is related to the total depth of penetration by a factor of about 7.5.

For both the Vickers and the Berkovich indenters, the representative strain within the specimen material is approximately 8% (see Sect. 1.3).

2.3.4 Cube Corner Indenter

The Berkovich and Vickers indenters have a relatively large face angles, which ensures that deformation is more likely to be described by the expanding cavity model rather than slip-line theory, which is equivalent to saying that the stresses beneath the indenter are very strongly compressive. In some instances, it is desirable to indent a specimen with more of a cutting action, especially when intentional radial and median cracks are required to measure fracture toughness. A cube corner indenter offers a relatively acute face angle that can be beneficial in these circumstances. Despite the acuteness of the indenter, it is still possible to perform nanoindentation testing in the normal manner and the expression for the projected area of contact is the same as that for a Berkovich indenter where in this case the face angle is $\theta = 35.26^\circ$:

$$\begin{aligned} A &= 3\sqrt{3}h_c^2 \tan^2 \theta \\ &= 2.60h_c^2 \end{aligned} \quad (2.15)$$

The equivalent cone angle for a cube corner indenter evaluates to 42.278° . The ratio of the length of a side of the residual impression to the total penetration depth is approximately 2.6. That is, the size of the impression on the surface is about 2.6 times as large as the total penetration depth.

2.3.5 Knoop Indenter

The Knoop indenter is similar to the Vickers indenter except that the diamond pyramid has unequal length edges, resulting in an impression that has one diagonal with a length approximately seven times the shorter diagonal [3]. The angles for the opposite faces of a Knoop indenter are 172.5° and 130° . The Knoop indenter is particularly useful for the study of very hard materials because the length of the long diagonal of the residual impression is more easily measured compared to the dimensions of the impression made by Vickers or spherical indenters.

As shown in Fig. 2.4, the length d of the longer diagonal is used to determine the projected area of the impression. The Knoop hardness number is based upon the projected area of contact and is calculated from:

$$KHN = \frac{2P}{d^2 \left[\cot \frac{172.5}{2} \tan \frac{130}{2} \right]} \quad (2.16)$$

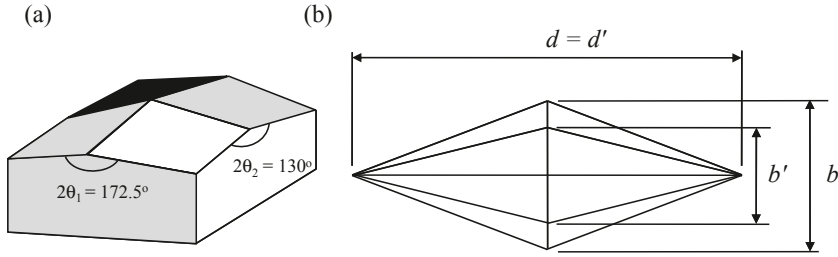


Fig. 2.4 (a) Geometry of a Knoop indenter. (b) The length of the long diagonal of the residual impression remains approximately the same from full load to full unload. The size of the short diagonal reduces from b to b' due to elastic recovery during unloading

For indentations in highly elastic materials, there is observed a substantial difference in the length of the short axis diagonal for a condition of full load compared to full unload. Marshall, Noma, and Evans [4] likened the elastic recovery along the short axis direction to that of a cone with major and minor axes and applied elasticity theory to arrive at an expression for the recovered indentation size in terms of the geometry of the indenter and the ratio H/E :

$$\frac{b'}{d'} = \frac{b}{d} - \alpha \frac{H}{E} \quad (2.17)$$

In Eq. 2.17, α is a geometry factor found from experiments on a wide range of materials to be equal to 0.45. The ratio of the dimension of the short diagonal b to the long diagonal d at full load is given by the indenter geometry and for a Knoop indenter, $b/d = 1/7.11$. The primed values of d and b are the lengths of the long and short diagonals after removal of load. Since there is observed to be negligible recovery along the long diagonal, then $d' \approx d$. When H is small and E is large (e.g. metals), then $b' \approx b$ indicating negligible elastic recovery along the short diagonal. When H is large and E is small (e.g. glasses and ceramics), then $b' \ll b$. Using measurements of the axes of the recovered indentations, it is possible to estimate the ratio E/H for a specimen material using Eq. 2.17.

The equivalent cone angle for the Knoop indenter is 77.64° . The projected area of contact is given by:

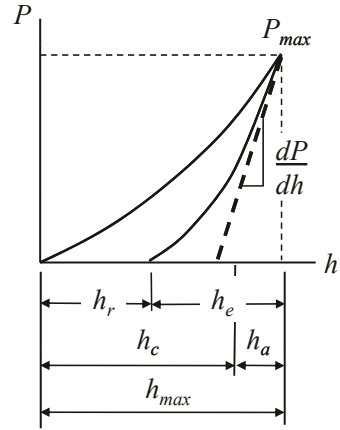
$$A = 108.21 h_c^2 \quad (2.18)$$

The ratio of the length of the long diagonal to the total penetration depth is 30.5.

2.4 Load-Displacement Curves

The principal goal of nanoindentation testing is to extract elastic modulus and hardness of the specimen material from experimental readings of indenter load and depth of penetration. In a typical test, force and depth of penetration are recorded as

Fig. 2.5 Compliance curves, loading and unloading, from a nanoindentation experiment with maximum load P_{max} and depth beneath the specimen free surface h_{max} . The depth of the contact circle h_c and slope of the elastic unloading dP/dh allow specimen modulus and hardness to be calculated. h_r is the depth of the residual impression, and h_e is the displacement associated with the elastic recovery during unloading



load is applied from zero to some maximum and then from maximum force³ back to zero. If plastic deformation occurs, then there is a residual impression left in the surface of the specimen. Unlike conventional indentation hardness tests, the size (and hence the projected contact area) of the residual impression for nanoindentation testing is too small to measure accurately with optical techniques. The depth of penetration together with the known geometry of the indenter provides an indirect measure of the area of contact at full load, from which the mean contact pressure, and thus hardness, may be estimated. When load is removed from the indenter, the material attempts to regain its original shape, but it prevented from doing so because of plastic deformation. However, there is some degree of recovery due to the relaxation of elastic strains within the material. An analysis of the initial portion of this elastic unloading response gives an estimate of the elastic modulus of the indented material.

The form of the compliance curves for the most common types of indenter are very similar and is shown in Fig. 2.5. For a spherical indenter, it will be shown in Chap. 5 that the relationship between load and penetration depth for the loading portion for an elastic–plastic contact is given by:

$$h = \frac{1}{2} \left(\frac{P}{\pi R_i H} + \frac{3}{4} \frac{\sqrt{P\pi H}}{\beta E^*} \right) \quad (2.19)$$

For the elastic unloading, we have from Eq. 1.7:

$$h = \left[\frac{3}{4E^* R^{1/2}} \right]^{2/3} P^{2/3} \quad (2.20)$$

³ Generally we use the term “load” to indicate that which is applied to the indenter, and “force” to that which is measured by the force sensor. In some instruments, it is the load applied that is recorded, while in others (which have a force sensor), it is the force that is measured. Ideally load and force would be identical and so either term can be used.

For a Berkovich indenter, it will be shown in Chap. 5 that the expected relationship between load and depth for an elastic–plastic contact is given by:

$$h = \sqrt{P} \left[(3\sqrt{3}H \tan^2 \theta)^{-\frac{1}{2}} + \left[\frac{2(\pi - 2)}{\pi} \right] \frac{\sqrt{H\pi}}{2\beta E^*} \right] \quad (2.21)$$

Upon elastic unloading we have from Eq. 1.13:

$$h = \sqrt{P} \left(\frac{\pi}{2E^*} \right)^{\frac{1}{2}} \left(\frac{\pi}{3\sqrt{3}} \right)^{\frac{1}{4}} \frac{1}{\tan \theta'} \quad (2.22)$$

where in Eqs. 2.20 and 2.22 the quantities R' and θ' are the combined radii and angle of the indenter and the shape of the residual impression in the specimen surface. The dependence of depth on the square root of the applied load in Eqs. 2.19–2.22 is of particular relevance. This relationship is often used in various methods of analysis to be described in Chap. 3.

In subsequent chapters, the methods by which elastic modulus and hardness values are obtained from experimental values of load and depth are described along with methods of applying necessary corrections to the data. In most cases, methods of analysis rely on the assumption of an elastic–plastic loading followed by an elastic unloading—with no plastic deformation (or “reverse” plasticity) occurring during the unloading sequence.

The indentation modulus is usually determined from the slope of the unloading curve at maximum load. Equation 2.23 shows that the indentation modulus (here expressed as E^*) as a function of dP/dh and the area of contact.

$$E^* = \frac{1}{2} \frac{\sqrt{\pi}}{\sqrt{A}} \frac{dP}{dh} \quad (2.23)$$

The indentation hardness is calculated from the indentation load divided by the projected contact area.

$$H = \frac{P}{A} \quad (2.24)$$

The contact area in turn is determined from the value of h_c (see Fig. 1.3) and the known geometry of the indenter (Table 1.1). The value for h_c is found by an analysis of the load-displacement data (see Fig. 2.5).

Variations on the basic load–unload cycle include partial unloading during each loading increment, superimposing an oscillatory motion on the loading, and holding the load steady at a maximum load and recording changes in depth. These types of tests allow the measurement of viscoelastic properties of the specimen material.

In practice, nanoindentation testing is performed on a wide variety of substances, from soft polymers to diamond-like carbon thin films. The shape of the load-displacement curve is often found to be a rich source of information, not only for providing a means to calculate modulus and hardness of the specimen material, but also

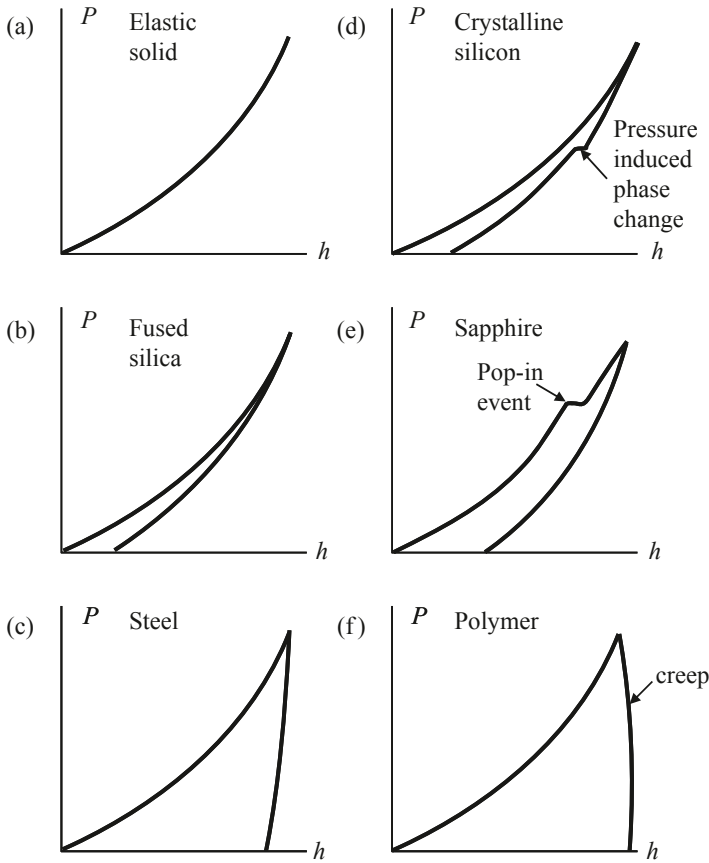


Fig. 2.6 Schematic examples of load-displacement curves for different material responses and properties. (a) Elastic solid, (b) brittle solid, (c) ductile solid, (d) crystalline solid, (e) brittle solid with cracking during loading, and (f) polymer exhibiting creep

for the identification of non-linear events such as phase transformations, cracking, and delamination of films. Figure 2.6 shows a schematic of some of the more commonly observed phenomena. It should be noted that in many cases the permanent deformation or residual impression is not the result of plastic flow but may involve cracking or phase changes within the specimen.

2.5 Experimental Techniques

Despite the mature evolution of nanoindentation test instruments, the process of undertaking such a test requires considerable experimental skill and resources. Such tests are extremely sensitive to thermal expansion from temperature changes and

mechanical vibration during testing. It is necessary to ensure that the specimen and the instrument are in thermal equilibrium. For example, handling the specimen or the indenter requires a reasonable delay before beginning the indentation so that errors are not introduced into the displacement measurements by virtue of thermal expansion or contraction during the test. Should there be any long-term thermal drifts, then these should be quantified and the appropriate correction made (see Chap. 4). In this section, specified matters requiring attention in practical indentation tests are summarized and commented upon.

2.5.1 Instrument Construction and Installation

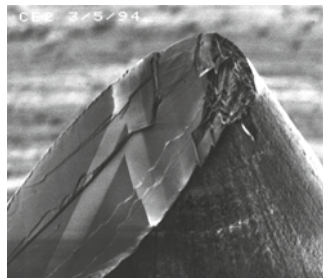
The nanoindentation instrument should be insulated against temperature variation, vibration, and acoustic noise in normal laboratory conditions. A specially designed enclosure designed to reduce thermal and electrical interference to a minimum is usually supplied by the manufacturer as part of the installation. For very low penetration depths (< 100 nm) an active vibration mounting may be required.

The loading column and base of a nanoindentation instrument should be of heavy construction so as to act as a seismic mass (to reduce the transmission of mechanical vibration) and to have a very high compliance (to minimize the effect of reaction forces on the displacement readings). The indenter is typically mounted on a shaft that is made from stiff, yet lightweight material to minimize compliance and maximize the resonant frequency of the system (the latter condition being important for dynamic indentation testing).

Specimens are typically mounted on a metal base with wax or mounting adhesive. The specimen holder is in turn placed on a stage. Stage movement is usually controlled by motorized axes that have a resolution, or step size, of less than $0.5\text{ }\mu\text{m}$. Such fine positioning is usually needed to allow indentations to be made on very small features such as grains in a ceramic or conductive pads in an integrated circuit. Stage movement is usually servo controlled with proportional, integral, and derivative gains that can be set to allow for the most precise positioning. Optical rotary or linear track encoders are usually employed. The encoder is usually mounted on the lead screw of the axis drive and a high-quality ball nut drives converts rotary motion to linear motion of the stage. Backlash in this nut is negligible. The operating software allows automatic positioning of the specimen beneath the indenter.

Load is typically applied to the indenter shaft by an electromagnetic coil or the expansion of a piezoelectric element. Displacements are usually measured using either a changing capacitance or inductance signal. Most nanoindentation instruments are load controlled, that is, a commanded force is applied and the resulting displacement is read. A detailed discussion on the features of instrument design is given in Chap. 11.

Fig. 2.7 Brittle failure of a 2 μm radius sphero-conical indenter. (Courtesy CSIRO)



2.5.2 Indenters

Diamond indenters are very hard, but also very brittle and can easily be chipped or broken (see Fig. 2.7). The mechanical properties of diamond differ according to the orientation of the measurement due to the crystalline nature of the diamond structure. Literature values for modulus range from about 800 GPa to 1200 GPa. A value of ≈ 1000 GPa is usually used in the analysis of nanoindentation test data with a Poisson's ratio of 0.07.

The indenter must be absolutely clean and free from any contaminants. Diamond indenters are most effectively cleaned by pressing them into a block of dense polystyrene. The chemicals in the polystyrene act as a solvent for any contaminants and the polystyrene itself offers a mechanical cleaning action that is not likely to fracture the indenter. The indenter itself should be attached to the indenter shaft firmly and in such a manner so as to minimize its compliance—this is often a matter for the manufacturer of the instrument.

The choice of indenter is important and depends upon the information one wishes to obtain from the indentation test. The representative strain in the specimen material, for geometrically similar indentations such as that made by Vickers and Berkovich indenters, depends solely on the effective cone angle of the indenter. The sharper the angle, the greater the strain. According to Tabor, the representative strain for a conical indenter is given by:

$$\varepsilon = 0.2 \cot \alpha \quad (2.25)$$

which for a Berkovich and Vickers indenter, evaluates to about 8%. If larger strains are required, say, for example, to induce cracking or other phenomena, then a sharper tip may be required. The representative strain for a cube corner indenter evaluates to about 22%. Indentations made with sharp indenters induce plasticity from the moment of contact (neglecting any tip-rounding effects). This may be desirable when testing very thin films in which the hardness of the film, independent of the substrate is required.

Spherical indenters offer a gradual transition from elastic to elastic-plastic response. The representative strain varies as the load is applied according to:

$$\varepsilon = 0.2 \frac{a}{R} \quad (2.26)$$

It is important that when measuring hardness using a spherical indenter, a fully developed plastic zone is obtained. In metals, this usually corresponds to a value for a/R of greater than 0.4. The changing strain throughout an indentation test with a spherical indenter enables the elastic and elastic-plastic properties of the specimen to be examined along with any strain-hardening characteristics.

2.5.3 Specimen Mounting

Test specimens must be presented square on to the axis of the indenter and held firmly with the absolute minimum of compliance in the mounting (Fig. 2.8). Typically, a specimen is mounted onto a hardened base or specimen mount using a very thin layer of glue. Holding devices such as magnets, vacuum chucks or spring clamps may be used.

The working range of a typical nanoindentation instrument is usually in the order of microns and so the specimen surface, if many indentations are to be made, is required to be parallel with the axis of translation. A departure from parallelism of about 25 μm over a 10 mm traverse can typically be tolerated by an instrument.

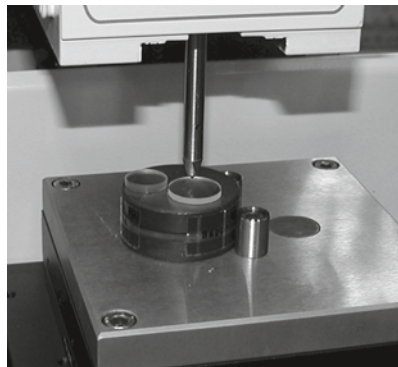
If a polishing technique is employed to prepare a surface, the properties of the surface material may be altered (see Sect. 4.11). Indentations placed on scratches, inclusions, or voids will give unpredictable results.

2.5.4 Working Distance and Initial Penetration

A typical nanoindentation instrument has a limited range of displacement over which the indentation depth may be measured. It is therefore necessary to ensure that the full range of the depth measurement system is available for measuring penetration depth into the specimen and not used for bringing the indenter into contact with the surface from its initial parked position. Usually, the measurement head of the instrument is allowed to translate vertically in coarse steps until the indenter is within 100 μm or so of the specimen surface. This is called the “working distance” and ensures that most of the available high-resolution displacement occurs during the final approach to the surface and the subsequent penetration into the specimen.

Once the measurement head has been set so that the indenter is at the working distance, it is then necessary to bring the indenter down to touch the surface with the minimum possible contact force. This becomes the reference position for any subsequent displacement readings. The minimum contact force is a very important measurement of performance for a nanoindentation instrument. No matter how small the minimum contact force is, it will result in some penetration into the specimen surface that has to be corrected for in the final analysis. Of course, if the initial penetration is too large, then it is possible that the indenter will penetrate past the surface layer or film desired to be measured. In many respects, the specification of the minimum contact force is the parameter that distinguishes a nanoindentation instrument from a microindentation instrument.

Fig. 2.8 Example of a fused silica specimens of diameter ≈ 10 mm mounted on a cylindrical hardened steel specimen mount and placed into position on a servo-motor-driven X-Y positioning stage. In this instrument, magnets firmly clamp the specimen mount to the stage. (Courtesy Fischer-Cripps Laboratories)



Some nanoindentation instruments apply the initial contact force by bringing the indenter down at a very small velocity until a preset initial contact force is measured by a separate force sensor. Others monitor the “stiffness” of the contact by oscillating the indenter shaft and noting when the oscillations undergo a sudden reduction in amplitude. The process can be automated so that it becomes independent of the operator. The initial contact force is typically in the range of $5 \mu\text{N}$ or less.

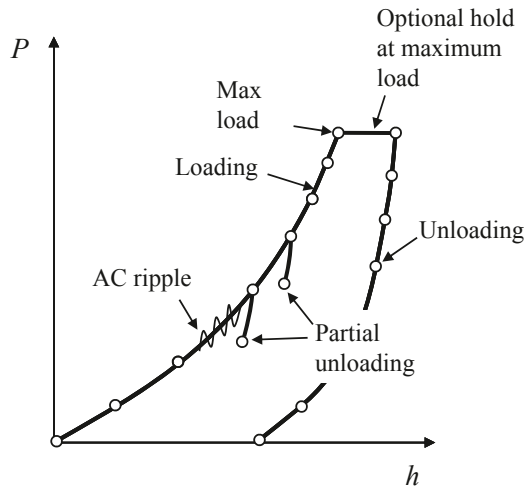
2.5.5 Test Cycles

A typical nanoindentation test cycle consists of an application of load followed by an unloading sequence—but there are many variations. Load may be applied continuously until the maximum load is reached, or as a series of small increments. At each load increment, a partial unloading may be programmed that provides a measurement of stiffness of the contact (dP/dh), which is important for measuring changes in modulus or hardness with penetration depth. Contact stiffness may also be found by superimposing a small oscillatory motion onto the load signal.

The indentation instrument may be set into either load or depth control. In load control, the user specifies the maximum test force (usually in mN) and the number of load increments or steps to use. The progression of load increments may be typically set to be a square root or linear progression. A square root progression attempts to provide equally spaced displacement readings. In depth control, the user specifies a maximum depth of penetration. It should be noted that most nanoindentation instruments are inherently load-controlled devices, but true load and depth control is available if there is a feedback loop employed which can take a signal from either a force or displacement sensor.

It is customary for a nanoindentation instrument to allow for a dwell or hold period at each load increment and at maximum load. The dwell settings at each load increment allow the instrument and specimen to stabilize before depth and load readings are taken.

Fig. 2.9 Various components of a nanoindentation test cycle



Hold period data at maximum load can be used to measure creep within the specimen or thermal drift of the apparatus during a test. Hold measurements for the purposes of thermal drift are probably best carried out at the end of the indentation test, at a low load, so as to minimize any effects from creep within the specimen. Figure 2.9 summarizes the loading, hold and unloading periods in a typical test cycle.

References

1. E.S. Berkovich, "Three-faceted diamond pyramid for micro-hardness testing," *Ind. Diamond Rev.* 11 127, 1951, pp. 129–133.
2. B.R. Lawn, *Fracture of Brittle Solids*, 2nd Ed., Cambridge University Press, Cambridge, 1993.
3. F. Knoop, C.G. Peters, and W.B. Emerson, "A sensitive pyramidal-diamond tool for indentation measurements," Research Paper 1220, *Journal of Research, National Bureau of Standards*, 23 1, 1939.
4. D.B. Marshall, T. Noma, and A.G. Evans, "A simple method for determining elastic-modulus-to-hardness ratios using Knoop indentation measurements," *J. Am. Ceram. Soc.* 65, 1980, pp. C175–C176.

Nanoindentation

Fischer-Cripps, A.C.

2011, XXII, 282 p., Hardcover

ISBN: 978-1-4419-9871-2